Control challenges for extremely large telescopes

Douglas G. MacMartin

Douglas G. MacMartin, "Control challenges for extremely large telescopes," Proc. SPIE 5054, Smart Structures and Materials 2003: Industrial and Commercial Applications of Smart Structures Technologies, (14 August 2003); doi: 10.1117/12.484661

SPIE.

Event: Smart Structures and Materials, 2003, San Diego, California, United States

Control Challenges for Extremely Large Telescopes

Douglas G. MacMartin

Department of Control and Dynamical Systems
California Institute of Technology
Pasadena CA 91125

ABSTRACT

The next generation of large ground-based optical telescopes are likely to involve a highly segmented primary mirror that must be controlled in the presence of wind and other disturbances, resulting in a new set of challenges for control. The current design concept for the California Extremely Large Telescope (CELT) includes 1080 segments in the primary mirror, with the out-of-plane degrees of freedom actively controlled. In addition to the 3240 primary mirror actuators, the secondary mirror of the telescope will also require at least 5 degree of freedom control. The bandwidth of both control systems will be limited by coupling to structural modes. I discuss three control issues for extremely large telescopes in the context of the CELT design, describing both the status and remaining challenges. First, with many actuators and sensors, the cost and reliability of the control hardware is critical; the hardware requirements and current actuator design are discussed. Second, wind buffeting due to turbulence inside the telescope enclosure is likely to drive the control bandwidth higher, and hence limitations resulting from control-structure-interaction must be understood. Finally, the impact on the control architecture is briefly discussed.

Keywords: Extremely Large Telescopes, CELT, Segmented Mirror Control

1. INTRODUCTION

The current generation of ground-based optical telescopes have primary mirrors with an effective aperture of 8-10 m. The largest monolithic primary mirrors are 8.2 m in diameter; to exceed this size, the twin 10 m Keck telescopes use segmented primary mirrors whose alignment is actively controlled.[1,2] Various designs are underway for the next generation of "Extremely Large Telescopes" (ELT's) with effective apertures of 30 m or more. All of these designs involve a highly segmented primary mirror, resulting in a new set of control challenges. The initial design for the 30-meter diameter California Extremely Large Telescope[3] (CELT) has 1080 hexagonal segments, as illustrated in Figure 1. The out-of-plane degrees of freedom will be actively controlled by 3240 actuators using feedback from 6204 edge sensors; the geometry is similar to that of the Keck telescopes, but with 30 times more actuators. The point design for the 30-meter Giant Segmented Mirror Telescope[4] (GSMT) involves 618 segments, while the 50-meter Euro50[5] uses 618 larger segments. Even larger telescopes are being considered such as OWL,[6] and future designs with many more segments have also been considered.[7] The choice of segment size is the result of a cost optimization, with smaller segments resulting in more control hardware; this trade-off is described in detail in the references for each of the point designs mentioned above. Clearly, with thousands of actuators, cost and reliability of the control hardware is a critical issue.

Current generation telescopes use active control to maintain the figure of the primary mirror, whether it is monolithic or segmented. However, the bandwidth of these control systems is intended to compensate only for gravity- and thermal-induced deformations. It is expected that wind-induced deformations will be larger for the larger telescopes,[8–11] and that the bandwidth of the control system will need to increase to compensate. Furthermore, the larger structures will have lower resonant frequencies. Thus, in addition to having many more actuators and sensors, the control bandwidth may be sufficient to interact with flexible structural modes. Further understanding of this problem requires development of models of wind turbulence inside telescope enclosures[9,12] as well as attention to the control-structure interaction problem.[13]

All of the ELT designs mentioned above, CELT, GSMT, Euro50 and OWL, also differ from current generation optical telescope designs in the support structure for the secondary mirror; a tripod feedleg structure is used

Smart Structures and Materials 2003: Industrial and Commercial Applications of Smart Structures Technologies, Eric H. Anderson, Editor, Proceedings of SPIE Vol. 5054 (2003) © 2003 SPIE · 0277-786X/03/$15.00

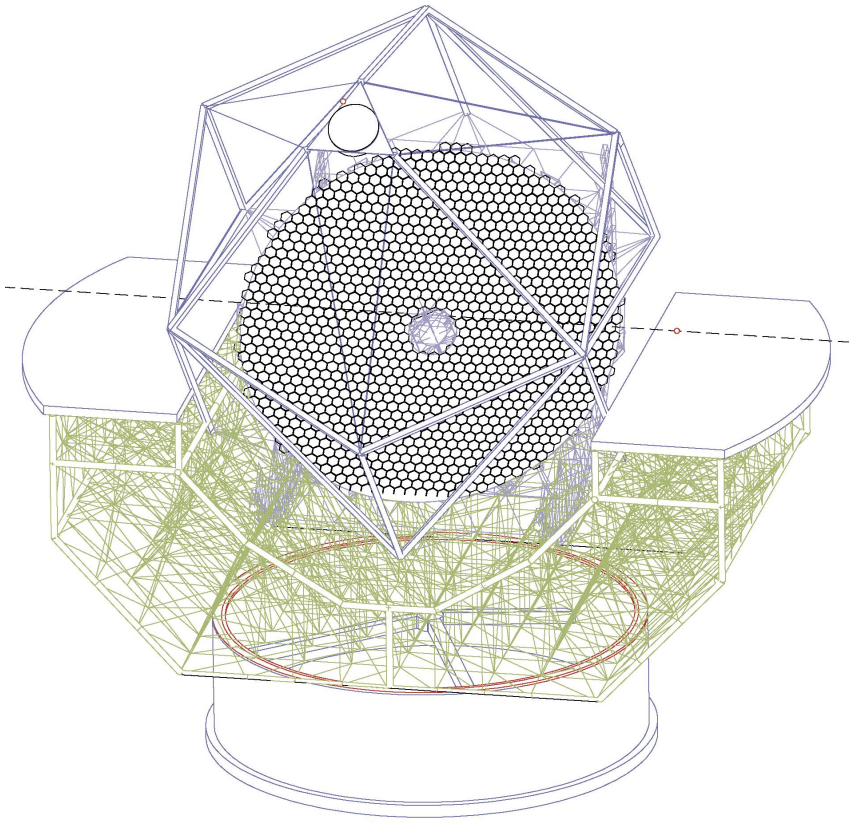

Figure 1. The CELT design, from Ref. 3, showing the 1080 hexagonal segments of the 30 m primary mirror.

in place of a spider supported secondary mounted on a telescope tube. The secondary position will need to be actively controlled to compensate for both gravity and wind loads. Furthermore, the loads on the secondary structure can couple into the primary mirror causing further optical distortions.[11,14]

Broadly speaking, there are three main control challenges faced in developing active optics systems for the next generation of extremely large, 30 m or larger optical telescopes:

1. The cost and reliability associated with several thousand actuators and sensors presents a design challenge. The actuators require a large stroke but high precision.

2. Wind-induced deformations are likely to require compensation, resulting in a potential interaction between the control and structural modes. The dynamic wind buffeting needs to be understood, the control designed in the presence of uncertain modes, and the limits to control bandwidth understood.

3. Tip/tilt and figure errors can be corrected using control at the primary mirror, the secondary, or by the adaptive optics system; the trade-off as a function of spatial and temporal bandwidth needs to be understood.

In addition to controlling tip/tilt and figure errors of the primary and secondary mirror (active optics), any future observatory will be designed with the potential for adaptive optics (AO) to compensate for atmospheric distortion. This allows a significant increase in scientific capability by enabling near-diffraction-limited resolution. Adaptive optics for ELT's adds its own set of control challenges that have been documented elsewhere,[15–17] requiring significant advances in end-to-end modeling, component technology development, and algorithms. Because the number of actuators required scales with the collecting area, such systems for ELT's may require 20 000 or more

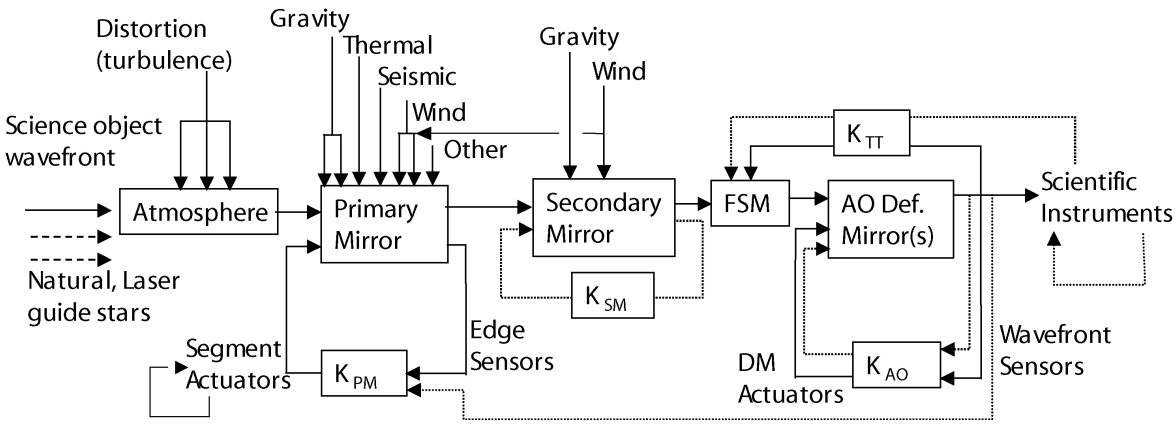

Figure 2. Block diagram for CELT wavefront propagation indicating disturbances (entering from the top of the figure) and control loops (mostly shown below the wavefront propagation path), adapted from Ref, 22. The control architecture shown is decentralized, although this is not required.

actuators in a multi-conjugate configuration,[18] resulting in a significant real-time computational burden that requires algorithmic improvements.[19]

The challenges associated with telescope active optics will be discussed in the subsequent sections, using the initial point design for CELT, described in detail in the conceptual design study.[3] Previous papers describe the preliminary design concepts for the active control hardware for CELT,[20] and preliminary analysis of the control problem for CELT,[21–23] as well as the control archictecture for GSMT.[13,14,24]

2. CONTROL PROBLEM

CELT will operate in two modes, seeing-limited (without adaptive optics), and (nearly) diffraction-limited (with adaptive optics). The goal for seeing-limited observations is to degrade atmospheric seeing by less than 10%, leading to a goal for the telescope to contribute $\theta(80) < 0.26$ arcseconds to the 80% enclosed-energy diameter,[3] of which 53 milli-arcseconds (mas) is allocated for control errors, including actuator noise, the error in desired sensor readings, sensor noise, and residual vibration above the control bandwidth. Similarly, to not significantly degrade adaptive optics performance, the diffraction-limited error budget is 50 nm rms of un-correctable wavefront error due to all telescope sources, of which 17.8 nm is allocated to errors from the active control system. Low wavenumber distortions of the primary mirror can be corrected by the adaptive optics system provided that this does not result in saturation of the AO actuators, while segment edge discontinuities cannot be well corrected by a smooth deformable mirror.

The wavefront propagation, disturbances, and (decentralized) control loops are shown in Figure 2. Disturbances include atmospheric turbulence distorting the wavefront; gravity, thermal, seismic and wind influences on the primary mirror; and gravity and wind influences on the secondary mirror. The main elevation and azimuth axes for pointing of the telescope are not explicitly shown in the figure. In addition to the main axes, there are 3 groups of control actuators; primary mirror segment actuation, secondary mirror rigid body actuation, and deformable mirrors (possibly including the secondary).

The three out-of-plane degrees of freedom of each mirror segment are actively controlled, resulting in 3240 actuators for the current CELT design, compared with 108 for the 36-segment Keck telescopes. Figure (shape) control uses feedback from "edge" sensors mounted across each inter-segment gap that measure the relative displacement between neighbouring segments (see Figure 3 for the geometry), and possibly wavefront information, although edge sensors are likely to be sufficient.[23] The secondary mirror (M2) position must be actively controlled in at least five degrees of freedom. In addition, the figure of the secondary is likely to be actively controlled at low bandwidth, and in both the GSMT and Euro50 designs, the secondary mirror is adaptive (a thin face-sheet mirror controlled by distributed actuation) and used as an element of the adaptive optics system.

3. CONTROL HARDWARE

The cost and reliability of the control hardware for the primary mirror is a significant concern. Because of the fewer components in the position control of the secondary, this system has received minimal attention to date. The M2 actuation requirements (stroke, bandwidth) will follow from a more detailed consideration of the wind loading and resulting structural deformation. The actuators themselves are likely to follow from the technology used in recent telescope designs; the secondary mirror actuators for positioning and chopping at Keck II[25] and at Gemini[26] both employ voice-coils.

The relative displacement of neighbouring segments is measured using capacitive edge sensors. This approach has proven successful at Keck, and the sensor noise at low frequencies[23] is less than $1\,\mathrm{nm}^2/\mathrm{Hz}$. A redesigned sensor is planned for CELT.[20]

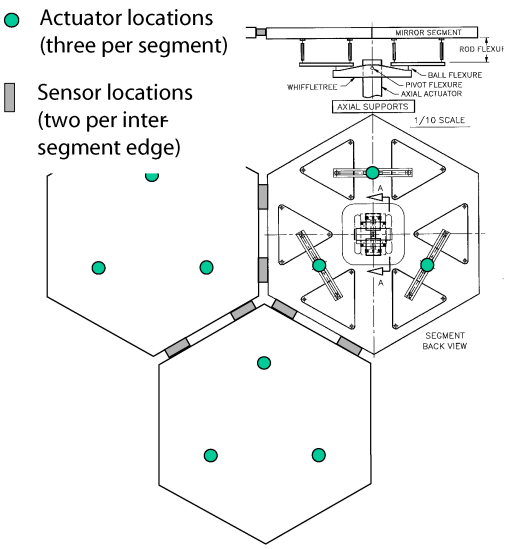

Figure 3. Schematic of sensor and actuator arrangement on mirror segments. The upper right segment shows the distribution of forces over the mirror through the whiffle tree. (The inter-segment gap is greatly magnified for clarity.) From Ref. 22.

The key requirements for the primary mirror actuators are illustrated in Table 1. The stroke requirement is derived from the maximum deflection of the mirror under gravity, and the precision requirement is set to minimize optical errors; the factor of 300,000 between these is a significant design challenge. Stiffness is required to avoid too low a segment support resonance frequency. The telescope is inoperable with a single actuator failure, and therefore extremely high reliability is required; the target MTBF of 10^3 years corresponds to an actuator failure roughly every 4 months. Finally, cost is, of course, a significant concern. The actuators used at Keck (see Figure 4) use a roller-screw driven by a stepper motor through a gearbox, with the roller screw output applied through a 24:1 hydraulic lever to achieve sufficient precision, about 4 nm per step. However, the cost and reliability are inadequate for the number of actuators required of an ELT.

An initial survey of actuator technologies was conducted early in the conceptual design stage of CELT,[27] and the broad categories of options are discussed in Ref. 22. The roller-screw technology used in Keck could undoubtedly be used successfully, but better and more economical solutions are now available. Several promising technologies were identified as a result of the survey and developed further. The option currently being considered as the primary solution is a two-stage voice-coil actuator[28] shown in Figure 4. The voice-coil provides the required precision, with a high bandwidth control loop to obtain the desired stiffness, and a low bandwidth large stroke actuator is used to off-load the voice-coil. Other options have also been developed to meet the specifications of ELT's.[29]

Stroke	$\geq 2.4\,\mathrm{mm}$
Precision	$\leq 7\,\mathrm{nm}$
Slew rate	$\geq 10\,\mu\mathrm{m/s}$
Transverse load capacity	$\geq 5\,\mathrm{kg}$
Axial load capacity	$\geq 30\,\mathrm{kg}$
Transverse stiffness	$\geq 0.1\,\mathrm{N}/\mu\mathrm{m}$
Axial stiffness	$\geq 10\,\mathrm{N}/\mu\mathrm{m}$
Local power dissipation	$\leq 2\,\mathrm{W}$
Lifetime (MTBF)	$\geq 10^3$ years
Cost target	$\simeq$ \$2000
Operating temperature	-6 to +10 °C

Table 1. CELT primary mirror actuator requirements, from Ref. 3.

Two-stage actuators are an attractive way to simultaneously achieve the desired precision and stroke, as each actuator can be made significantly cheaper. For the telescope application, the large stroke motion is required to compensate for gravitational deflection, and hence the offload can be implemented passively with a suitable counterweight. Different active, passive, and hybrid active/passive offload schemes are discussed in detail in Ref. 28. The recommended design uses a hybrid active/passive offload, and a lever system to reduce the forces required for both the voice-coil and the offload system.

Once a two-stage or offload approach is chosen, then the actuator design becomes one of selecting the precision actuator technology. Two obvious choices are voice-coil (such as used in existing secondary mirror actuation)

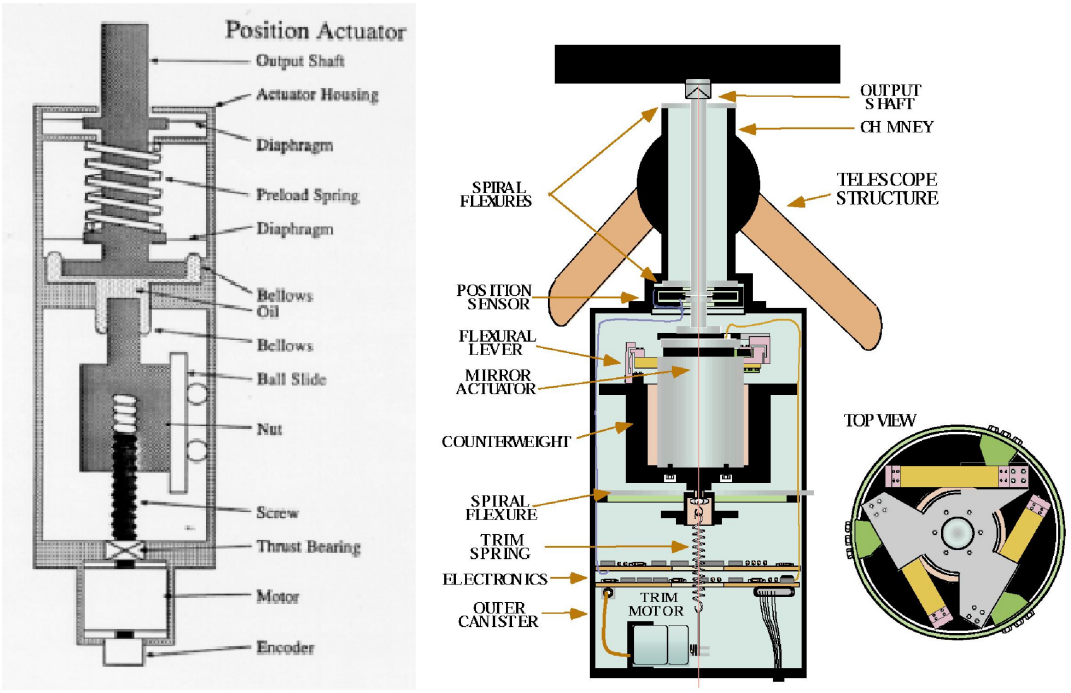

Figure 4. Keck roller screw actuator with hydraulic motion reduction mechanism (left), from Ref. 1, and potential CELT voice coil actuator with offload mechanism (right) from Ref. 28.

or piezoelectric (or other solid state actuation). The former requires a sensor and a feedback loop to achieve the desired stiffness, but offers the advantage of being able to provide some passive damping to the segment resonance mode. Voice-coils are also cheap and reliable, making this an attractive solution. The solid state actuation requires minimal power to hold a given position. However, we expect the precision actuation to have to respond constantly to compensate for wind buffeting of the mirror, and therefore this is not a significant advantage.

The relative advantage of using a "soft" actuator such as the voice-coil and obtaining the stiffness electronically compared with a stiff actuator depends on the bandwidth of the local actuator control loop. Infinite stiffness at zero frequency is easy to obtain with an integral control law. However, for low control bandwidths, the effective dynamic stiffness is significantly reduced at frequencies where there may be sufficient wind excitation of the segment. For sufficiently high control bandwidth, there is no significant adverse effects from inadequate stiffness, and the control can be used to actively damp the segment support resonance. This effect is straightforward to model using a coupled oscillator, as shown in Figure 5. The nominal segment resonant frequency of 60 Hz is based on the whiffle-tree stiffness k_w, with 3 actuators supporting the $3m = 74\,\mathrm{kg}$ segment weight.

The nominal response of the mirror segment to an applied force (such as wind loads) when supported on the whiffle tree and an infinite stiffness actuator is

$$G_{\mathrm{nom}}(s) = (ms^2 + c_w s + k_w)^{-1} \tag{1}$$

where c_w is a nominal damping chosen to give $Q = 50$ for this mode. With x as the segment displacement and x_a as the displacement of the actuator, then the coupled system is described by:

$$m\ddot{x} + c_w(\dot{x} - \dot{x}_a) + k(x - x_a) = f \tag{2}$$

$$m_a\ddot{x}_a + c_a\dot{x}_a - c_w(\dot{x} - \dot{x}_a) + k_a x_a - k(x - x_a) = u \tag{3}$$

where m_a, k_a and c_a are the mass, stiffness, and damping of the actuator (none of which significantly influence the simulation). Choose the control as a PID with bandwidth ω_b (rad/sec)

$$u = Kx_a, \qquad K(s) = K_i/s + K_p + K_d s/(1 + s/\omega_r) \tag{4}$$

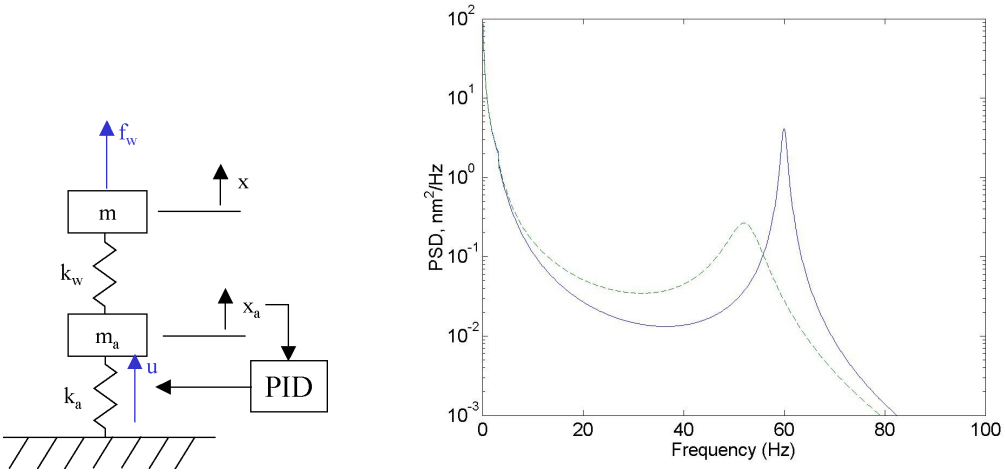

Figure 5. Schematic of mirror segment actuated by a "soft" actuator (left). The segment mass is supported on the whiffle tree stiffness k_w and actuator; the actuator stiffness is augmented through a PID loop. The mirror response x (right) with the controlled soft actuator (dashed line) is compared to that with an infinite stiffness actuator (solid line), both subjected to a wind disturbance from Eq'n (5).

with gains $K_i = m(\omega_b/2)^3$, $K_p = m\omega_b^2$, $K_d = \sqrt{2}m\omega_b$ and $\omega_r = 3\omega_b$. For a 100 Hz bandwidth, the response is shown in Figure 5, compared with the response with an infinitely stiff actuator. The disturbance is based on the wind model from Eq'n (5). The nominal whiffle tree resonance at 60 Hz is damped, and shifts to a lower frequency due to the finite actuator stiffness. In addition, the response at frequencies below the segment resonance is increased due to the decreased stiffness. Because the nominal resonant frequency is at a high enough frequency where there is minimal wind-induced vibration, the contribution from the resonance in the infinitely-stiff actuator case is small, and the benefit from active damping is relatively minor. In this case, the "soft" actuator provides a net improvement in performance provided that the bandwidth of the control loop is roughly equal to the nominal segment resonance or more. For lower control bandwidths, the increase in off-resonant response is greater than the benefit from damping the resonance.

The potential clearly exists for a smart-material based two-stage actuator, however, this must be competitive in cost, reliability, and performance with the voice-coil design in Figure 4; Lorell and Aubrun[28] estimate the cost of this actuator to be only about 10% higher than the cost target set in Table 1. The requirements on the precision stage follow from the stiffness requirement in Table 1 and the residual stroke not offloaded to the coarse stage. The maximum gravity deflection that must be compensated while tracking an object is 140 nm per second. Lorell and Aubrun[28] estimate that a 0.1 Hz bandwidth is possible for a simple offload motor; the resulting stroke requirement for the precision stage to compensate only for gravity is therefore roughly 1.4 μm. The estimate for the wind-induced vibrations has not yet been finalized, but a total 2 μm stroke is probably sufficient. If so, then a small PZT stack could readily provide both sufficient deflection and stiffness.

4. WIND-BUFFETING AND CONTROL BANDWIDTH

Although wind-buffeting is not a significant design driver for current generation telescopes, it is expected to be more significant for the larger ELT's due to the larger cross-sectional area, lower stiffness and lower structural resonant frequencies.[8–11] Although the telescope enclosure significantly reduces the wind speeds inside the dome relative to those outside the dome, the residual wind may still lead to telescope vibration and resulting unacceptable image blur if not compensated. The static wind loads can be readily compensated by a low bandwidth active control system, but the dynamic wind-induced vibration due to turbulence drives the control system bandwidth requirements, and/or yields a contribution to image blur due to uncorrected contributions.

The wind influences the telescope structure through three distinct paths: (i) loads on the secondary and secondary support structure causing motion of the secondary mirror, (ii) loads on the primary mirror deforming

the primary mirror, and (iii) loads on the secondary and secondary support structure that lead to deformations of the primary mirror through structural coupling. It is the third of these that is expected to be the most significant optical performance driver for ELT's.[11] In addition, there are wind forces on the Nasmyth platforms, and on the dome that can shake the telescope pier. Finally, note that some airflow within the dome is necessary to flush the enclosure and reduce the optical distortions that result from thermal variations. The wind speeds required to do so are not known, but are likely to be small.

The first step in modeling these effects is a model for the wind turbulence inside the telescope dome; this can be done computationally (e.g. DeYoung[12]) or empirically. The best source of data for this is a test conducted at the Gemini South Observatory involving 24 pressure transducers mounted on a dummy primary mirror, and five 3-axis anemometers, three around the primary, one near the secondary location, and one above the dome.[8,9,30] Five minute data records were collected at 10 Hz. The Gemini Observatory has wind vents that can be opened to flush the enclosure. Data was collected with the wind vents both open and closed; however, to estimate the worst-case wind buffeting only the cases with the vents fully closed are considered. This is based on the assumption that mitigating dome seeing does not require significant wind flow through the dome, and thus if wind speeds are sufficient to cause a buffeting problem, then the vents would be (nearly) closed. Anomolous data has been discarded, and there are relatively few remaining data sets from which to draw conclusions. Each data set corresponds to a different orientation relative to the wind or a different night, however, all of the orientations are within a 45° azimuth angle of the wind direction (elevation between 15 and 60° from zenith.)

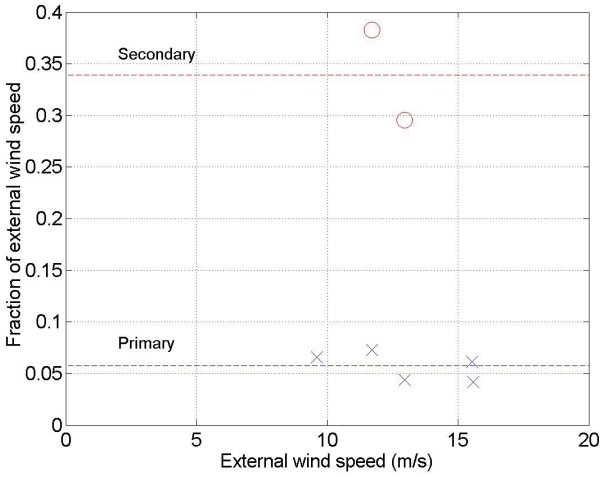

Figure 6. Influence of the dome on interior wind speeds, from Gemini data with vents closed. Each point corresponds to a different dome orientation relative to the wind. Data for the primary ('×') and secondary ('◯') mirror locations are shown.

The reduction in wind speed due to the dome is shown in Figure 6. The rms wind speeds at the secondary location are about 1/3 of the external wind speed, while the rms at the primary mirror is roughly 6% of the external wind speed. Most of the energy in the external wind is in the mean, while most of the energy over the primary is in the turbulence, and the energy at M2 is roughly equally split between the mean flow and the turbulence. The 36 m diameter Gemini dome has a 10 m opening, while the 90 m CELT dome has a 32.5 m opening; the ratio of opening to dome diameter D_o/D_d is therefore 30% larger, and one should expect higher wind speeds inside the CELT dome. Padin[11] has considered a model for this and predicts that the interior wind speeds should scale with $(D_o/D_d)^{2/3}$. For the 95$^{\text{th}}$ percentile wind on Mauna Kea of 14 m/s, this leads to estimates of 1/2 the external rms wind speed at the secondary location or 7 m/s, and 10% at the primary or roughly 1.5 m/s.

To predict the impact of wind turbulence over the structure, the spatial and temporal spectrum is required in addition to the amplitude. The measured spectrum of both the wind velocity and the pressure over the primary mirror is shown in Figure 7. The wind speed spectrum is averaged over 3 axes, 3 locations, and 7 data sets; it compares well with a Kolmogorov $f^{-5/3}$ power law. The outer scale appears to be roughly 0.05 Hz, which is consistent with the wind-crossing time for the mirror (roughly 0.5 m/s over an 8 m mirror). The corresponding plot for the wind spectrum at the secondary shows a similar trend, and is not shown. The pressure spectra are plotted normalized by an outer scale based on the rms wind speed over the primary $\langle v_p^2 \rangle^{1/2}$ and the mirror radius R_p. Each curve is the average spectrum over 24 pressure transducers. Also shown is a model based on fully developed turbulence. This model assumes $f^{-7/3}$ roll-off, with the outer scale based on the wind-crossing time of the mirror radius. Thus the pressure spectrum is of the form

$$\Phi(f) = \frac{A}{(1 + (fR_p)^2/\langle v_p^2 \rangle)^{7/6}} \tag{5}$$

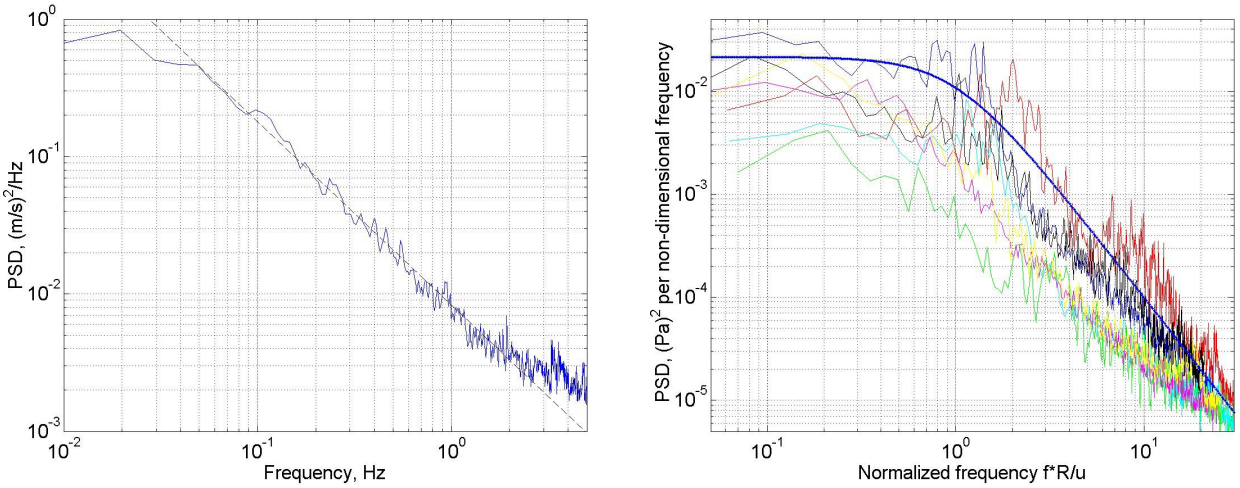

Figure 7. Spectrum of wind over primary (left) from Gemini South data with vents closed, averaged over 9 anemometer channels and 7 data sets; the spectrum is similar across data sets. The dashed line shows the comparison with the expected $f^{-5/3}$ power law. Spectrum of pressure over primary (right), averaged over 24 pressure transducers. Each curve represents a different data set, indicating differences in the pressure spectrum with telescope orientation. The thick line is a model spectrum obtained with a $f^{-7/3}$ power law and an outer scale based on the wind-crossing time for the mirror. The vertical scale is obtained from $v_p = .05 v_e$ and $p = 0.5\rho v_p^2$.

The amplitude of the model is scaled according to the results from Figure 6; the rms pressure is predicted from the external wind speed using the expected reduction in wind speed at the primary and computing dynamic pressure as $0.5\rho v_p^2$. While the model clearly does not correctly predict the details of the pressure spectrum, it does seem to be a reasonable approximation. Certain data sets show peaks in some frequency regions that may be associated with local vortex shedding over the structure.

Since the outer scale is determined by the scale length of the mirror (or the dome opening), it is reasonable to assume that the turbulence results primarily from either the flow passing through the opening, or from the interaction of the flow with the telescope structure, and is *not* related to the transport of the mountain-top boundary layer turbulence into the interior of the dome.

Estimates of the impact of wind buffeting on the telescope structure have been made both using the data directly[8,9,14] and using models motivated by the results discussed above.[10,11] For ELT's, based on simple structural models, the most significant impact is the excitation of the primary due to the wind loads on the secondary support structure coupling into the primary mirror support structure. The bandwidth of the disturbances is relatively low; for the worst-case wind, then the forces on the secondary start to decrease above roughly $f_0 = v/R \simeq 7/15 \sim 0.5\,\mathrm{Hz}$, while those on the primary decrease above $\sim 0.1\,\mathrm{Hz}$. With the spectrum in Eq'n 5, then roughly half the energy is below the corner frequency.

With a preliminary structural design,[3] the first flexible modes for CELT are currently roughly 1.6 and 1.9 Hz, changing to 1.2 and 1.6 Hz as the telescope points from zenith to 65°. Subsequent design refinements may increase these resonant frequencies, but probably by at most a factor of 2. The GSMT model shows 20 modes below 10 Hz.[13] Significant deflections are therefore possible not only through the quasi-static response, but through excitation of lightly damped structural modes. Active control of the primary mirror figure will be challenging at these frequencies. Although these first modes involve primarily tip and tilt of the primary, even control of higher order shapes will inevitably couple with these modes. Because of the variation in the mode frequency with orientation, any control algorithm with a bandwidth over low spatial frequencies that is more than a fraction of one Hz will require significant complexity to avoid deleterious structural interaction. As a result, we expect to use the position of the secondary mirror to compensate for at least some of the tip/tilt deflections of the primary mirror, as discussed in the following section.

Higher spatial wavenumber control, required to maintain segment continuity, will not couple strongly to these first few telescope modes, and may achieve much higher bandwidths. These errors can only be corrected at the primary mirror, but there is also much less energy in the wind disturbance at these higher spatial frequencies. Assume frozen turbulence so that the spatial spectrum is similar to the temporal spectrum in Eq'n (5). Then integrating yields that the energy in all spatial scales shorter than 1 m is roughly 1.5% of the total wind energy. The rms inter-segment edge discontinuity results from the pressure that is decorrelated between neighbouring segments and can thus be calculated from the worst-case total rms pressure $\rho v_p^2/2$, the segment area of $0.65\,\mathrm{m}^2$, the residual energy at high wavenumber, and the segment support stiffness. The last factor assumes a 75 kg segment mass and a 60 Hz resonant frequency, so $K \simeq 10^7\,\mathrm{N/m}$. This yields an rms wavefront error of 21 nm, roughly half of which could be corrected by the adaptive optics system. The residual energy at the scale of individual segments is small even for a worst-case wind assumption. Nonetheless, for risk reduction it is reasonable to maintain as high a bandwidth as possible at each spatial scale, since there is no cost to doing so.

5. CONTROL ARCHITECTURE

Figure 2 in Section 2 implies that the primary mirror K_{PM}, secondary mirror K_{SM} and adaptive optics loops are independent, however, there is clearly the possibility to share information (as implied by the wavefront information being possibly used by K_{PM}) or for a correction to take place at a location other than where the wavefront error is introduced. Deflections due to gravity are slow and predictable. A feedforward algorithm and very low bandwidth feedback is sufficient to compensate for this disturbance. Thermally induced deflections are similarly slow and easy to compensate. However, wind-induced vibrations may require a more complex, and potentially coupled compensation, due to the coupling of the control with structural modes as discussed in the previous section.

The control architecture may also depend on whether the telescope is operating with adaptive optics or in a seeing-limited mode, because the performance metric, the available information, and the available actuators all change. In particular, wavefront information is of minimal value in seeing-limited mode.[23] Provided that laser guide stars are available to obtain near-complete sky coverage, then the only reason for observing without adaptive optics is to take advantage of the field of view of the telescope. Over any significant field of view, the atmosphere is decorrelated, and atmospheric turbulence in the direction of the guide star is "noise" on the wavefront measurement. As the goal of the active optics control is to obtain telescope performance small compared to the atmospheric turbulence, this information is clearly not useful. However, if one is conducting observations with adaptive optics, then one is only using the field of view over which the atmosphere is correlated. In this case, wavefront information is already in use for the AO system.

The simplest control architecture is decentralized; the deformations of each mirror (primary, secondary, and any AO deformable mirrors) are controlled by actuation and sensing local to the corresponding system. This may be sufficient to decouple the adaptive optics system from the telescope active optics system. However, the primary and secondary mirror control systems are more naturally coupled. In particular, tip/tilt of the primary cannot be rapidly compensated due to interaction with telescope structural modes (see Section 4). The secondary mirror active control system can be more readily designed to be decoupled from the telescope modes (e.g. by moving a counterweight), and therefore a higher bandwidth should be possible. Thus the secondary position will likely be used to compensate for primary mirror tip/tilt errors that are above the feasible bandwidth of the primary mirror control system. If the secondary mirror has actuators for figure control, then additional low spatial wavenumber deformations of the primary mirror could also be offloaded. Conversely, if the secondary mirror is designed without figure control actuation, then predicted gravity-induced (slow) deformation of the secondary mirror surface could be compensated for using the primary mirror actuation. Similarly, in observations with adaptive optics on, there is the potential to control low wavenumber telescope deformations using AO deformable mirrors.

A hypothetical trade of control authority with spatial and temporal frequency is plotted in Figure 8. This is adapted from the similar plot in References 13,14. The telescope main azimuth and elevation axes are controlled at low bandwidth by systems similar to current telescopes. The secondary mirror (M2) position is controlled at higher frequencies, and is used to control the tip/tilt of the primary mirror (M1) at temporal frequencies higher than the M1 control can react. The primary mirror figure control bandwidth is expected to depend on spatial scale; high spatial wavenumber modes involving segment edge discontinuity can be controlled at higher

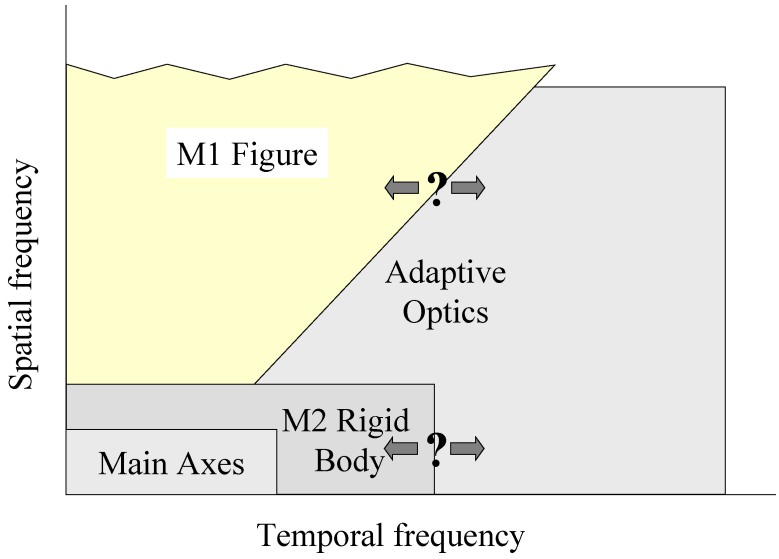

Figure 8. Authority of different control loops as a function of spatial and temporal bandwidth, adapted from Ref. 14. Higher bandwidth should be possible for higher wavenumber modes of the primary mirror control. Although there are finite degrees of freedom, the maximum wavenumber of the primary mirror control is infinite due to the edge discontinuities. The maximum bandwidth of either the primary mirror or secondary mirror loops has not yet been determined.

bandwidth due to the decreased coupling with global telescope modes. This ensures that the mirror surface is smooth, which is critical for successful adaptive optics performance.

The achievable bandwidth of both the primary and secondary mirror control systems has not yet been determined; this depends on three factors: the extent to which control of a given spatial shape can be decoupled from low frequency structural modes, the damping in those modes, and the degree of complexity in the control system. Parameterizing the control algorithm to adjust to one or two modes that change with the elevation angle of the telescope is plausible, or possibly adapting the controller; however, it is unlikely that such a strategy could be successful with many uncertain modes in the roll-off region of the controller.

6. CONCLUSIONS

The next generation of extremely large optical telescopes that are currently being considered will present several control challenges. These include effort in three main areas.

Because of the large number of segments, the control hardware must be low cost and very reliable. Recent work has proposed a design that appears to meet the requirements. The design uses a two-stage system, with a voice-coil to provide sufficient precision, and an active/passive off-load to reduce the stroke required of the voice-coil. A solid state actuator could also be used to provide the precision motion.

Unlike current generation optical telescopes, it is expected that wind buffeting of the telescope structure will excite structural resonances and cause sufficient vibration to degrade image quality if left uncompensated. Data collected at the Gemini South Observatory by the New Initiatives Office of AURA have been used to validate a simple model of the wind speeds and spectra inside the telescope enclosure, these in turn can be applied to simplified structural models of the telescope to predict the amplitude and frequency of motions requiring correction by the control system. To compensate for this, the control bandwidth should be increased as much as possible. The limiting factor on achievable control bandwidth will be interaction with uncertain structural modes whose mode shapes and frequencies may depend on telescope orientation.

The adaptive optics and telescope active optics controllers are likely to be decoupled. However, control of the primary and secondary mirrors are likely to be coupled. The primary mirror control bandwidth will be limited

by interaction with structural modes, and hence the secondary position will be used to compensate for higher frequency tip/tilt errors of the primary mirror.

Adaptive optics for extremely large telescopes also represents a significant challenge in many areas; these challenges have not been discussed in detail herein, but are extensively documented elsewhere.

ACKNOWLEDGEMENTS

Many of the results discussed herein were developed with the entire CELT project team, led by Jerry Nelson at the University of California, Santa Cruz. Jerry Nelson and Terry Mast (UCSC) led the effort on actuator hardware, and the voice-coil design presented was developed by Ken Lorell and Jean-Noel Aubrun. Discussions on control architecture involved Steve Padin (California Institute of Technology), and also George Angeli (AURA New Initiatives Office) and Mark Whorton (NASA Marshall Space Flight Center), both working on GSMT. The Gemini South Wind data from which the analysis in Figures 6 and 7 was developed was made available by the New Initiatives Office of AURA Inc. Discussions on wind modeling have involved both AURA and individuals working on CELT.

REFERENCES

1. Jared, R. C. *et al.*, "The W. M. Keck Telescope segmented primary mirror active control system," *SPIE* **1236** *Advanced Technology Optical Telescopes IV*, 1990, pp. 996–1008.
2. Cohen, R., Mast, T., and Nelson, J., "Performance of the W. M. Keck Telescope Active Mirror Control System," *SPIE* **2199**, 1994, pp. 105–116.
3. Nelson, J., and T. Mast, eds., *Conceptual Design for a 30-meter Telescope*, No. 34, CELT, 2002. Available at `http://celt.ucolick.org`.
4. Strom, S. E., Stepp, L., and Gregory, B., "Giant Segmented Mirror Telescope: a point design based on science drivers," *Astronomical Telescopes and Instrumentation*, 2002. SPIE Vol. 4840?
5. Andersen, T., Ardeberg, A., Beckers, J., Goncharov, A., Owner-Petersen, M., Riewaldt, H., Snel, R., and Walker, D., "The Euro50 Extremely Large Telescope," *Proc. SPIE* **4840**, 2002.
6. Dierickx, P., Delabre, B., and Noethe, L., "OWL Optical Design, Active Optics, and Error Budget," *SPIE* **4003**, (Munich), 2000.
7. Padin, S., "Design considerations for a highly segmented mirror," *Applied Optics*, Vol. 42, No. 10, 2003.
8. Cho, M. K., Stepp, L., and Kim, S., "Wind buffeting effects on the Gemini 8m primary mirrors," *SPIE* **4444**, *Optomechanical Design and Engineering* (Hatheway, A., ed.), 2001.
9. Cho, M. K., Stepp, L. M., Angeli, G. Z., and Smith, D. R., "Wind loading of large telescopes," *Large Ground-Based Telescopes* (Oschmann, and Stepp, eds.), 2002, pp. 352–367. Proc. SPIE **4837**.
10. Padin, S., "Wind-induced Deformations in a Segmented Mirror," *Applied Optics*, Vol. 41, No. 13, pp. 2381–2389, 2002.
11. Padin, S. and Davison, W., "A model of image degradation due to wind buffeting in a Cassegrain telescope," submitted to *Applied Optics*, 2002.
12. DeYoung, D. S., "Numerical Simulations of Airflow in Telescope Enclosures," *The Astronomical Journal*, Vol. 112, No. 6, pp. 2896–2908, Dec. 1996.
13. Whorton, M. and Angeli, G., "Modern control for the secondary mirror of the Giant Segmented Mirror Telescope," *Future Giant Telescopes* (Angel, and Gilmozzi, eds.), 2002. Proc. SPIE **4840**.
14. Angeli, G. Z., Cho, M. K., and Whorton, M. S., "Active optics and control architecture for a Giant Segmented Mirror Telescope," *Future Giant Telescopes* (Angel, and Gilmozzi, eds.), 2002. Proc. SPIE **4840**.
15. Rigaut, F., Ragazonni, R., Chun, M., and Mountain, M., "Adaptive Optics Challenges for the ELTs," *Proceedings of the Backaskog Workshop on Extremely Large Telescopes*, 1999, pp. 168–174. ESO Conference and Workshop Proceedings no 57.
16. LeLouarn, M., Hubin, N., Sarazin, M., and Tokovinin, A., "New Challenges for adaptive optics: extremely large telescopes," *Mon. Not. R. Astron. Soc.*, Vol. 317, pp. 535–544, 2000.
17. Goncharov, A. V., Owner-Petersen, M., Andersen, T., and Beckers, J. M., "Adaptive optics schemes for future extremely large telescopes," *Opt. Eng.*, Vol. 41, No. 5, pp. 1065–1072, May 2002.

18. Dekany, R., Bauman, B., Gavel, D., Troy, M., Macintosh, B., and Britten, M., "Initial Concepts for CELT Adaptive Optics," *SPIE* **4840**, 2002.
19. Ellerbroek, B. L., "Efficient computation of minimum-variance wave-front reconstructors with sparse matrix techniques," *J. of the Optical Society of America A*, Vol. 19, No. 9, pp. 1803–1816, 2002.
20. Mast, T. and Nelson, J., "Segmented Mirror Control System Hardware for CELT," *SPIE* **4003**, 2000.
21. Chanan, G., Nelson, J., Ohara, C., and Sirko, E., "Design Issues for the Active Control System of the California Extremely Large Telescope (CELT)," *Telescope Structures, Enclosures, Controls, Assembly/Integration/Validation, and Commissioning* (Sebring, T. A., and T. Andersen, eds.), 2000, pp. 363–372. Proc. SPIE **4004**.
22. MacMartin, D. G., Mast, T. S., Chanan, G., and Nelson, J. E., "Active Control Issues for the California Extremely Large Telescope," *Guidance, Navigation, and Control Conference*, AIAA, 2001. AIAA 2001-4035.
23. MacMartin, D. G. and Chanan, G., "Control of the California Extremely Large Telescope Primary Mirror," *Astronomical Telescopes and Instrumentation*, 2002. SPIE Vol. 4840.
24. Chung, S.-J., Miller, D. W., Angeli, G. Z., and Ellerbroek, B. L., "Optimal control of adaptive optics and active optics for a future telescope with dynamic reconstruction," submitted to *AIAA Guidance Navigation and Control Conference*, 2003.
25. Aubrun, J.-N., Lorell, K. R., Feher, G. J., Perez, E. O., Reshatoff Jr., P. J., and Zacharie, D. F., "Design of the infrared fast steering mirror chopping control system for the Keck II telescope," *Advanced Technology Optical/IR Telescopes VI*, 1998, pp. 687–698. Proc. SPIE **3352**.
26. Lorell, K. R., Aubrun, J.-N., Perez, E. O., Reshatoff Jr., P. J., and Zacharie, D. F., "Test and performance evaluation of the Gemini secondary mirror chopper and position control system," *Advanced Technology Optical/IR Telescopes VI*, 1998, pp. 699–710. Proc. SPIE **3352**.
27. Schier, A., "Summary of the CELT Mirror Segment Actuator Survey," CELT Technical Report 15, 2001. Available at `http://celt.ucolick.org`.
28. Lorell, K. R. and Aubrun, J.-N., "Primary Mirror Actuators Phase I Study Report," CELT Technical Report 18, 2001. Available at `http://celt.ucolick.org`.
29. Nalbandian, R. and Hatheway, A. E., "Extra Large Telescope Actuator (ELTA)," *Large Ground-Based Telescopes* (Oschmann, J. M., and L. M. Stepp, eds.), 2002, pp. 814–820. Proc. SPIE **4837**.
30. Smith, D. R., "Gemini South Wind Tests," 2001. Available at `http://www.aura-nio.noao.edu/studies/wind_tests1/index.html`.